THE JOURNAL OF PHYSICAL CHEMISTRY C

Article

pubs.acs.org/JPCC

Theoretical Analyses on Phosphorescent Processes in $Pt(thpy)_2$ and Its Derivatives

Shiro Koseki,*[,†,§] Yuhki Kagita,[†] Sachiko Matsumoto,[†] Toshio Asada,[†,§] Shigayuki Yagi,[‡,§] Hiroyuki Nakazumi,[‡,§] and Takeshi Matsushita[§,∥]

[†]Department of Chemistry and [‡]Department of Engineering, Graduate School of Science, Osaka Prefecture University, 1-1 Gakuen-cho, Sakai, Osaka 599-8531, Japan

[§]The Research Institute for Molecular Electronic Devices (RIMED), Osaka Prefecture University, 1-1 Gakuen-cho, Naka-ku, Sakai 599-8531, Japan

[∥]JNC Petrochemical Corporation, 5-1 Goikaigan, Ichihara, Chiba 290-8551, Japan

Supporting Information

ABSTRACT: Theoretical estimation of the peak wavelengths of phosphorescence was performed at the MCSCF+SOCI/SBKJC+p level of theory for several typical platinum complexes in the research field of organic-light-emitting-diodes (OLEDs), where MCSCF +SOCI is the abbreviation of multiconfiguration self-consistent field calculations followed by second-order configuration interaction calculations. The spin−orbit coupling (SOC) integrals among low-lying electronic states of different spin multiplicities were explicitly calculated within the Z_{eff} approximation. By using these computational methods, the experimental results for peak wavelengths of phosphorescence were reasonably explained for *cis*-bis[2-(2′-thienyl)pyridinato-N,$C_{3'}$]platinum(II) and its derivatives. The replacement of one of the 2-(2′-thienyl)pyridinate (*thpy*) ligands by a 2,4-pentanedionate (*acac*) ligand causes a blue shift of the phosphorescent peak by about 10 nm. The use of a 1,3-bis(phenyl)propane-1,3-dionate (*bpp*), 1,3-bis(*n*-methoxyphenyl)propane-1,3-dionate (*bmp*), or 1,3-bis(3,4-methoxyphenyl)propane-1,3-dionate (*bdmp*) ligand, instead of an *acac* ligand, has almost no effect on the peak wavelength of phosphorescence. When a benzene ring is fused to a *thpy* ligand, the peak wavelength is estimated to be 613 or 651 nm for [2,2′-(4′,5′-benzo)thienyl)pyridinato-N,$C_{3'}$][1,3-bis(3,4-dibutoxyphenyl)-propane-1,3-dionato-O,O]platinum(II) [*btp*Pt(bdbp)] and [1-(2′-thienyl)isoquinolyl-N,$C_{3'}$][1,3-bis(3,4-dibutoxyphenyl)-propane-1,3-dionato-O,O]platinum(II) [*1tiq*Pt(bdbp)], respectively, after correction of the present computational underestimation. These theoretical estimations are in good agreement with the corresponding observations.

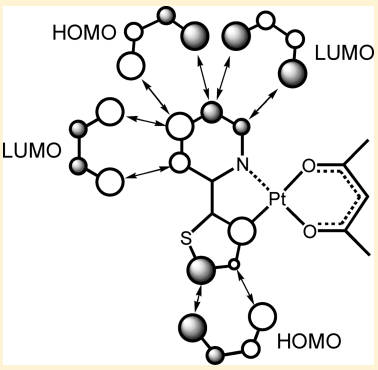

INTRODUCTION

Much attention has recently been paid to organic electroluminescent panels or organic-light-emitting-diode (OLED) panels as the next generation of display devices, although liquid crystal flat panels are now widely used as television and personal computer monitors. OLED panels are also considered to be useful as room lights for special purposes (so-called white OLEDs). Unfortunately, most OLED panels provide fluorescence and have a relatively low quantum yield of electroluminescence (internal yield of 25% at most). It is apparent that phosphorescence should be used in the fabrication of more efficient devices, since the internal yield of phosphorescence could reach 75% statistically and even to 100% on the basis of a fast intersystem crossing from singlets to triplets or by harvesting both fluorescent and phosphorescent emissions. However, generally speaking, it is difficult to obtain efficient phosphorescence in pure organic molecules at room temperature,[1−15] even though pure organic molecules efficiently emit phosphorescence at a low temperature. There have been many reports on platinum and iridium complexes, since these complexes are considered to be the most applicable candidates in this research field,[16−67] but it is still considered that brighter and long-life emissive materials should be proposed as three-color devices.

At the first stage of our research projects, the parent molecules bis[2-(2′-thienyl)pyridinato]platinum [$Pt(thpy)_2$] and tris(2-phenylpyridinato)iridium [$Ir(ppy)_3$] were theoretically investigated with respect to their emission processes.[65−67] Although most of the theoretical investigations employed density functional theory (DFT) and/or time-dependent DFT (TDDFT), we employed the multiconfiguration self-consistent field (MCSCF) method[68] in order to optimize the molecular orbitals and to explicitly calculate spin−orbit coupling (SOC) effects in these complexes. During the past three decades, our research group has performed theoretical investigations of the SOC effects in monohydrides of first- through third-row transition elements[69−71] within one-electron approximation, effective nuclear charge approximation, or Z_{eff} approximation of

Received: May 12, 2014
Revised: June 19, 2014
Published: June 20, 2014

   dx.doi.org/10.1021/jp5046832 | J. Phys. Chem. C 2014, 118, 15412−15421

the Breit−Pauli (BP) Hamiltonian.[72] This theoretical method was applied to the study of the low-lying potential energy surfaces in di- and tetrahydrides of third-row transition elements.[73−76] It is noteworthy that the SOC effects play important roles in the dissociation paths of rhenium tetrahydride into rhenium dihydride and a hydrogen molecule.[76] It should be stated here that, because of the use of effective core potentials (ECPs) and their associated basis sets, the full BP Hamiltonian provides small values for SOC integrals and that, therefore, Z_{eff} approximation needs to be employed in order to reproduce experimentally obtained results. Although we proved that the combination of all-electron basis sets and the full BP Hamiltonian can provide reasonable results,[77−83] it is quite time-consuming to apply to large OLED complexes including many-electron heavy elements. We also examined model core potentials (MCPs) and their associated basis sets, together with the full BP Hamiltonian, and obtained results similar to the corresponding ECP results.[66]

On the basis of such experiences, we started theoretically explaining the experimental results for the OLED complexes from the viewpoint of SOC effects.[65−67] In our first paper of this research series,[65] the differences between $Pd(thpy)_2$ and $Pt(thpy)_2$ were analyzed and explained theoretically. Another parent molecule, $Ir(ppy)_3$, was the target in our second paper. Since this molecule is too large to perform MCSCF calculations with high reliability, the MCSCF active space needed to be rather small: six electrons in six orbitals because of the limitation of our computer resources. Despite such difficulties, the calculated results could explain the experimental results within an acceptable systematic gap between the calculated and corresponding experimental results.

Encouraged by the success in explaining the phosphorescent processes in these parent complexes, theoretical calculations were performed for typical phosphorescent derivatives of $Ir(ppy)_3$.[67] The calculated results were in quantitative agreement with the corresponding experimental results within acceptable systematic gaps. That is to say, the calculated peaks of phosphorescence are mostly 15−30 nm shorter than the corresponding observed ones. In our previous paper, we proposed that the second stable geometrical isomer (homo-*cis*,hetero-N-*cis*) of FIrpic should be used for better blue-color phosphorescence, since it is higher than the most stable isomer (homo-*N*-*trans*) by only less than one kcal/mol.

Platinum complexes are four-coordinated and have less variety of ligand combinations than do Ir complexes, but they are still interesting as phosphorescent materials in the research field of OLEDs. We believe that the investigation of platinum complexes can provide some useful information for designing phosphorescent materials, especially for more cost-effective solution-processed OLEDs based on various printing techniques, instead of those for vapor deposition-processed ones. Thompson et al.[84−86] proposed soluble materials using heteroleptic (*C*^*N*)Pt(O^O) complexes. These complexes also have considerable advantages in their preparation and have been experimentally investigated by several research groups.[87−89] However, systematic theoretical investigations of such soluble phosphorescent materials for OLED devices have not yet been carried out.

In this research series, our investigations were performed only for isolated complexes. Recent developments of theoretical methods and computational techniques have made it possible to investigate the whole emissive layer of OLED devices by using the quantum mechanical/molecular mechanical molecular dynamic (QM/MM MD) simulation technique.[90−101] Such QM/MM MD simulations have been achieved in another series of our investigations,[96−101] while the present series of our theoretical investigations focuses on the behavior of a single complex, even though the interaction between the target complex and the host molecules in emissive layers could be very important.

The present paper focuses on providing theoretical explanations and suggestions for the design of better phosphorescent platinum complexes, since Yagi et al.[87−89] recently carried out systematic syntheses of various Thompson-type platinum complexes or heteroleptic (*C*^*N*)Pt(O^O) complexes and reported better materials for red-emission solution-processed OLEDs. In the next section, details of the theoretical methods of calculation are explained. In the third section, the emission processes in the parent molecule, bis[2-(2′-thienyl)pyridinato-N,$C_{3'}$]platinum(II) [$Pt(thpy)_2$] (**1** in Figure 1), are briefly reviewed first. Then a comparison is performed among $Pt(thpy)_2$ (**1**), [2-(2′-thienyl)pyridinato-N,$C_{3'}$][2,4-pentanedionato-O,O]platinum(II) [*thpy*Pt(acac)] (**2**), and the derivatives **3**−**7** and the effects of introducing a 2,4-pentanedionate (*acac*), 1,3-bis(phenyl)propane-1,3-dionate (*bpp*), 1,3-bis(*n*-methoxyphenyl)propane-1,3-dionate (*bmp*), or 1,3-bis(3,4-methoxyphenyl)propane-1,3-dionate (*bdmp*) ligand and the effects of a benzene ring fused to a 2-(2′-thienyl)pyridinate (*thpy*) ligand are theoretically analyzed on the basis of the discussion of these complexes (see Table S1 in the Supporting Information).

METHODS OF CALCULATION

The geometrical structures of the ground state (S_0) and the lowest triplet state (T_1) were optimized using a DFT method, where restricted and unrestricted Kohn−Sham orbitals are used for ground states and the lowest triplet states, respectively. In these calculations, the B3LYP functional[102] and the SBKJC effective core potentials and the associated basis sets[103,104] were used, being augmented by a set of polarization functions.[105] These basis sets are referred to as SBKJC+p in the present series of our investigations. In unrestricted DFT calculations, expectation values of the spin operator $\langle \hat{S}^2 \rangle$ were found to be maintained in the range of 2.010−2.053. These structures were examined by normal-mode analyses and were shown to be energy minima on the potential energy surfaces of the ground states or the lowest triplet states.

At these stationary geometries, the molecular orbitals were optimized using the multiconfiguration self-consistent field (MCSCF) method.[68] The MCSCF active space includes four electrons and four orbitals, two of the orbitals mainly having the Pt dπ character and the remaining two having the π^* character of each ligand (principally antibonding character) [MCSCF(4e,4)]. In order to equally optimize molecular orbitals for low-lying electronically excited states as well as the ground state, the state-averaging technique was employed; the lowest seven singlet and six triplet states were included in the averaging processes. Then second-order configuration interaction (SOCI) wave functions[106] were constructed using the MCSCF-optimized orbitals, where the external space included 200 external orbitals, which have the lowest eigenvalues of the standard MCSCF Fock operator, in the SOCI calculations with the aim of including electron correlation effects as much as possible. Since dπ orbitals mix moderately with ligands' π^* orbitals during MCSCF iteration, the present SOCI wave functions can explain ligand-to-ligand

dx.doi.org/10.1021/jp5046832 | J. Phys. Chem. C 2014, 118, 15412−15421

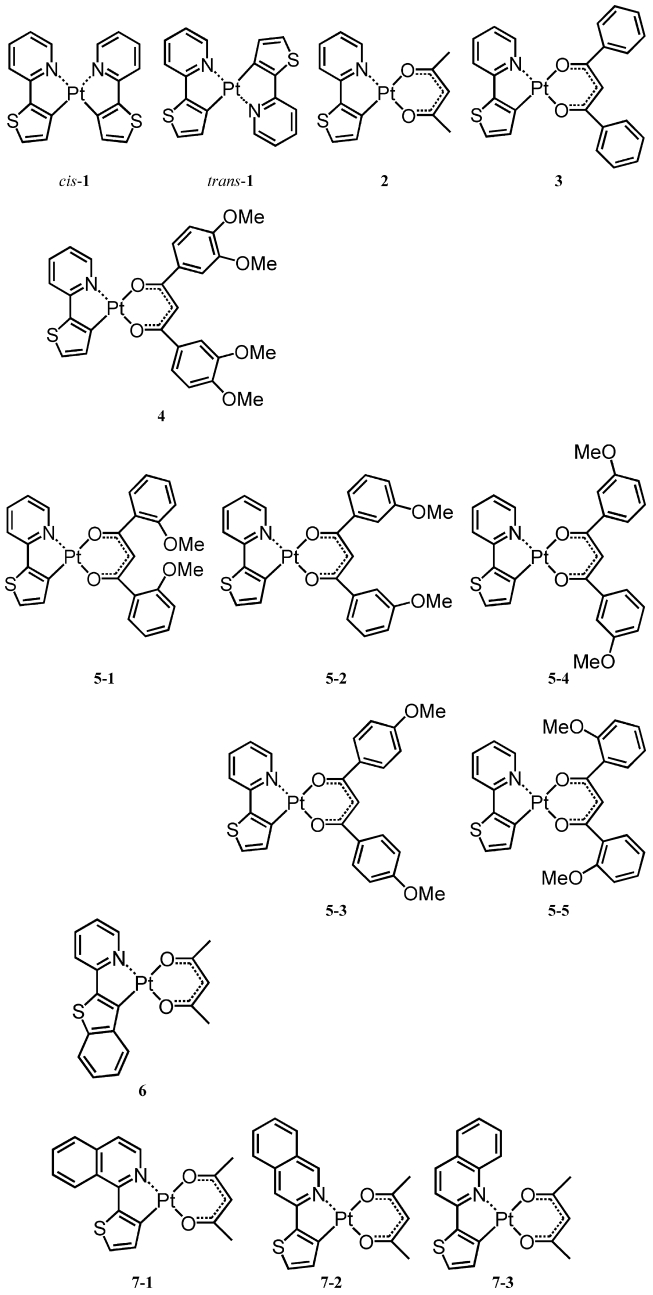

Figure 1. Geometrical structures of platinum complexes.

(π,π^*) charge transfer (LLCT) as well as metal-to-ligand (d,π^*) charge transfer (MLCT).

In order to explain intersystem crossings and phosphorescent processes, the SOC integrals between states of different spin multiplicities need to be estimated. For this purpose, the Breit–Pauli Hamiltonian was used in the SOC calculations. The SOC matrices include low-lying singlet, triplet, and quintet states, where the energy differences between the ground state and these target states should be smaller than 300 mhartree and higher multiplet states are not included because they are energetically high. Their matrix elements were computed within the Z_{eff} approximation,[77−83] where the numbers of configuration state functions included in the SOC calculations were 324420 (singlets), 443815 (triplets), and 120201 (quintets). All calculations were carried out using the GAMESS suite of program codes.[107]

Note that since the present investigation uses a set of natural orbitals optimized by the MCSCF method, the words "HOMO" and "LUMO" are inappropriate. However, for simplicity, these words will be used as our original definitions in the following discussion: HOMO means the natural orbital for which the occupation number (NOON) is *larger than one and the smallest* among them in the ground state, and LUMO means the natural orbital for which NOON is *smaller than one and the largest* among them in the ground state.

RESULTS AND DISCUSSION

1. Brief Review on the Parent Molecule 1. The parent molecule **1** (Figure 1, Figure S1 and Tables S1 and S2, Supporting Information) is well-known as a typical phosphorescent material of orange-color emission.[33−38,46] In our previous paper,[65] we reported the details of theoretical analyses of the emission processes in this complex: the geometrical structures of the ground state and the lowest triplet state were optimized for both *cis*-**1** and *trans*-**1** at the DFT (B3LYP) level of theory. Note that a set of *p* functions was not augmented for hydrogen atoms in our previous investigation,[65] but it was done in the present calculations. In order to estimate the spectral shape of phosphorescence, the wave functions of low-lying states in the *cis* isomer were constructed by using the MCSCF method followed by SOCI and SOC calculations, while the *trans* isomer was excluded from the investigation since it is thermally less stable than the *cis* isomer[108] (Table 1). Good agreement with results in available experimental reports[33−38,46] was obtained for this complex, as well as for analogous palladium complexes,[65] though the wavelengths of the spectral peaks were predicted to be underestimated by about 20 nm for the phosphorescent emission in *cis*-**1**.[33−38,46]

Table 1. Relative Energies (kcal/mol) of the Geometrical Isomers Optimized for Their Ground States at the DFT (B3LYP/SBKJC+p) Level of theory

molecule	DFT	MC	+SOCI	+SOC
cis-**1** $\{^1A\ (C_2)\}$	0	0	0	0
trans-**1** $\{^1A\ (C_2)\}$	7.5	5.7[a]	5.6[a]	5.6[a]
cis-**1** $\{^3A\ (C_2)\}$	50.1	66.3	70.7	70.7
cis-**1** $\{^3A\ (C_1)\}$[b]	44.9 (−5.3)	60.2 (−6.1)	64.6 (−6.1)	64.6 (−6.1)
5-1	8.6	8.2	8.0	8.0
5-2	2.5	2.4	2.2	2.2
5-3	0	0	0	0
5-4	2.1	2.5	2.3	2.3
5-5	10.0	8.6	9.0	9.0
6	0	0	0	0
7-1	4.8	9.1	9.8	9.8
7-2	4.2	15.6	11.7	11.7
7-3	8.5	11.1	11.5	11.5

[a]In *trans*-**1**, when the MCSCF active space includes two dπ orbitals (*b* symmetry), a higher total energy is obtained for the ground state, and as a result, the energy difference between *cis*-**1** and *trans*-**1** is calculated to be 28.5 (MCSCF), 26.1 (SOCI), or 25.5 (+SOC) kcal/mol. In the calculations shown in this table, one dσ orbital (a symmetry) and one dπ orbital (b symmetry) are included in the active space. [b]The stabilization energy caused by pseudo-Jahn–Teller distortion is shown in parentheses.

dx.doi.org/10.1021/jp5046832 | J. Phys. Chem. C 2014, 118, 15412−15421

Table 2. Comparison of Spectral Peak Wavelengths (nm) and Geometrical Displacements |ΔQ| (Å/Atom) Caused by the Electronic Transition between the Ground State and the Lowest Triplet State

molecule	peak wavelength[a] (nm)	TDM (e·bohr)	est wavelength (nm)	expt (nm)	ref	|ΔQ|
cis-**1** {^{3}A (C_2)}	545	0.0085	580	580/582	33−38, 49	0.044
trans-**1**	717	0.1832	752			0.343
2	533	0.0047	568	558−575	49, 50	0.039
3	546	0.0045	581			0.026
4	545	0.0046	580	560 (bdbp)	88	0.023
5-1	534	0.0049	569			0.026
5-2	537	0.0048	572			0.019
5-3	544	0.0046	579			0.020
5-4	538	0.0050	573			0.024
5-5	534	0.0052	569			0.021
6	565	0.0063	600	590−612	49, 50 87,−89	0.021
7-1	603	0.0052	638			0.024
7-2	531	0.0022	566			0.025
7-3	538	0.0055	573			0.025

[a]The main contribution is provided by the transition from the SM3 state to the ground state (SM0). The main adiabatic component of the SM3 state is T_1 in all complexes.

In our previous investigation,[65] the geometrical structures of the ground state (^{1}A) and the lowest triplet state (^{3}B) in both *cis* and *trans* isomers were found to have C_2 symmetry, while the planar structures (C_{2v} and C_{2h} structures, respectively) are apparently unstable. In the present investigation, geometrical optimization was carried out again, and the lowest triplet state in the *cis* isomer was found to be not the ^{3}B state but the ^{3}A state at the C_2 structure. Additionally, this lowest triplet state (^{3}A) at the *cis* isomer is calculated to be energetically lowered by geometrical deformation from C_2 symmetry to C_1 symmetry (Table 1). This geometrical deformation can be explained by pseudo-Jahn−Teller effects in the lowest ^{3}A state interacting strongly with low-lying ^{3}B states. Accordingly, in the following discussion, the deformed C_1 structure will be used for the lowest triplet state in order to calculate the emission spectra in the *cis* isomer. It was confirmed that the *trans* isomer has the lowest ^{3}B state and that the *trans* isomer maintains C_2 symmetry in the lowest triplet state.

Now, in order to reproduce experimental emission spectra, it is necessary to consider spectral broadening and anharmonicity caused by the interaction with its circumstances and the geometrical displacement between the energy minima of electronic states. In our laboratory, potential energy curves (PECs) for low-lying spin-mixed (SM) states were obtained along the geometrical displacement between the ground state and the lowest triplet state in order to estimate the spectral broadening caused by the anharmonicity of potential energy surfaces and the geometrical difference between the two electronic states. By using these PECs, vibrational wave functions were obtained in each SM state,[109] and the dependence of transition dipole moments (TDMs) on nuclear coordinates was calculated between vibrational states of the ground state (SM0) and several excited SM states.[110,111] However, it is too time-consuming to calculate the PECs of low-lying SM states in many complexes, and it becomes difficult to obtain the wave functions for energetically high vibrational states in each SM state. Therefore, we decided that the peak positions of emission spectra can be assumed to be provided by the superposition of Lorentz functions centered at the electronic transition energies from excited SM states to the ground state (SM0). In these calculations, the thermal population distribution for low-lying SM states was assumed to be given at an appropriate temperature, and a Lorentz function for each electronic transition was assumed to have an appropriate width. It took less time to calculate spectral shapes by using this method; since vibrational wave functions do not need to be obtained in each SM state. Table 2 lists only peak wavelengths and their initial states of the electronic transitions which mainly contributes to the spectral peaks, instead of illustrating the shapes of emission spectra.

We also decided to use an MCSCF active space different from that employed in our previous study, since spectral peaks have frequently been calculated to be longer than the corresponding experimental results. In that previous study, seven orbitals were included in the MCSCF active space, five of them principally having the Pt's dπ-orbital character and the other two primarily having the π^* character of each *thpy* ligand. Our analyses revealed that strong interaction occurs between metal and ligand π orbitals during MCSCF iteration, and as a result, dσ orbitals disappear from the MCSCF active space and pure ligand π orbitals appear instead. This situation causes overestimation of the π interaction in comparison with other interactions. This must be the reason why curiously long wavelengths were frequently obtained in our trial calculations of platinum complexes. Therefore, we decided that four orbitals, instead of seven orbitals, should be included in the MCSCF active space, two of them principally having the Pt's dπ character and the other two having the π^* character of each *thpy* ligand, as described in the previous section. Furthermore, since this new MCSCF active space is rather small, it was decided that 200 virtual orbitals were included in the external space of the SOCI calculations as described in the previous section.

The calculated results for *cis*-**1** are shown in Table 2. The spectral peak for this complex appears a the wavelength of 545 nm, which is shorter than the previous one (558 nm) and the corresponding observed one (580 nm) by 35 nm. This discrepancy seems large and must be caused by the small MCSCF active space, but as described in the following discussion, the new MCSCF active space gives us consistent results for all platinum complexes. On the other hand, the old larger MCSCF active space gave us a spectral peak of a long wavelength (592 nm) when the geometrical structure of the lowest triplet state is deformed to a C_1 symmetrical structure.

dx.doi.org/10.1021/jp5046832 | J. Phys. Chem. C 2014, 118, 15412−15421

Additionally, the SOC integrals were calculated to be relatively small. These results also must be caused by the small MCSCF active space. Since doubly occupied orbitals do not contribute to SOC integrals,[112−115] the number of open-shell configurations, which are thought to contribute to SOC effects, apparently becomes smaller as the active space becomes smaller. In fact, $\langle T_1(m_s = 1)|H_{SO}|S_0(m_s = 0)\rangle$ = 20 cm^{-1}, while it is 137 cm^{-1} when the old active space is used. Since Z_{eff} values were determined for the active space including all valence orbitals of molecules,[77−83] it may be necessary to determine them again using such a smaller active space. However, for simplicity, we decided to use the original Z_{eff} values, and we believe that the qualitative reliability should be reasonable.

The geometrical displacement between the lowest triplet state and the ground state was also calculated using our new definition.[67] The value would tell us how fast nonradiative transition occurs. Even after geometrical deformation from the C_2 structure to the C_1 structure occurs in the lowest triplet state in *cis*-**1**, the displacement is calculated to be small (|ΔQ| = 0.044 Å/atom). This is about eight times smaller than that in *trans*-**1** (|ΔQ| = 0.343 Å/atom), where the *trans* isomer maintains C_2 symmetrical geometry in the lowest state as mentioned above. Therefore, as already mentioned in our previous paper,[65] fast nonradiative transition occurs in *trans*-**1**, and it is understood that *trans*-**1** is inappropriate to use as an emissive material. Note that the present calculations provide a spectral peak at the wavelength of 701 nm in *trans*-**1** (Table 2).

2. Introducing a Soluble Ligand. As described in the Introduction, it is important to develop soluble complexes for low-cost printing devices. It is well-known that Thompson-type complexes are practical candidates.[84−86] The simplest target would be **2** (Figure 1). The calculated results for this complex are shown in Table 2. The spectral peak of the emission in this complex appears at the wavelength of 533 nm (SM3). In comparison with the calculated result (545 nm) for *cis*-**1**, the peak is shifted to a high energy region by about 12 nm. In *cis*-**1**, the LUMO is given by the linear combination of *thpy*'s π^* orbitals, while the LUMO is principally the π^* orbital of the *thpy* ligand in **2** (Figure 2). The π^* orbital of the *acac* ligand is explicitly higher in energy than that of the *thpy* ligand, so that the interaction between the π^* orbitals of *thpy* and *acac* ligands must be weaker than that between two *thpy* ligands in *cis*-**1**. The reason why the peak is slightly shifted to a high energy region must be weakening of the interaction strength between two ligands. The spectral peak was observed at the wavelength of 558−575 nm (depending on experimental conditions);[49,50] namely, the introduction of an *acac* ligand can be considered to cause a blue shift of 5−22 nm. Thus, it can be said that the present method gives us reasonable results with respect to the magnitude of spectral shift. Then, in the following discussion, the magnitude of the present computational underestimation is considered to be about 35 nm on the basis of the comparison between the calculated and experimental peak wavelengths for *cis*-**1** and **2**. Meanwhile, the geometrical displacement during the emission (between the lowest triplet state and the ground state) in **2** is calculated to be |ΔQ| = 0.039 Å/atom. Since this is comparable with that in *cis*-**1**, it can be understood that the nonradiative transition from the lowest triplet state to the ground state is not so fast in this complex.[49,50]

In practical syntheses,[49,50,87−89] larger ligands are usually used, but it is unfortunately impractical or too time-consuming to perform reliable theoretical predictions for complexes possessing such large ligands. Since the final target complex of the present study is set to [2,2′-(4′,5′-benzo)thienyl)-pyridinato-N,$C_{3'}$][1,3-bis(3,4-dibutoxyphenyl)propane-1,3-dionato-O,O]platinum(II) [*btp*Pt(bdbp)] reported by Yagi et al.[88] or its analogue [2,2′-(4′,5′-benzo)thienyl)pyridinato-N,$C_{3'}$]-[1,3-bis(3,4-dimethoxyphenyl)propane-1,3-dionato-O,O]-platinum(II) [*btp*Pt(bdmp)] (**4**), two kinds of effects on the spectral peaks were examined theoretically: (i) substituent effects on the *acac* ligand and (ii) effects of a benzene ring fused to the *thpy* ligand.

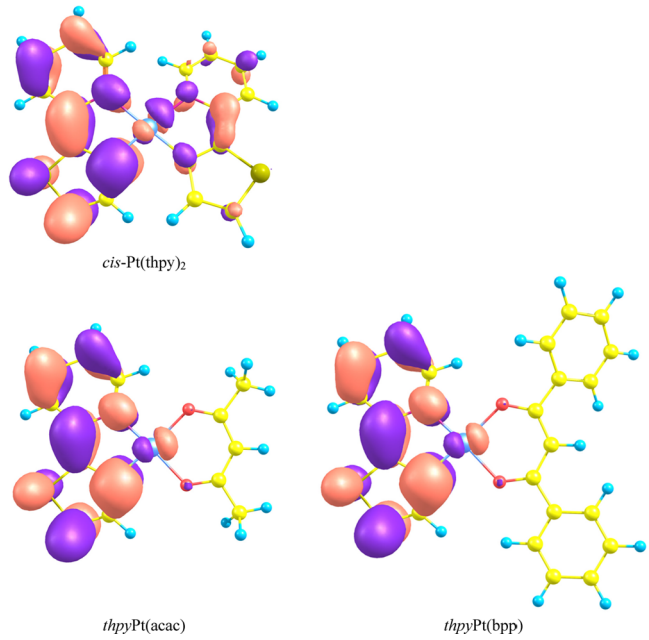

Figure 2. LUMOs in *cis*-Pt(thpy)$_2$, *thpy*Pt(acac), and *thpy*Pt(bpp).

2.1. Substituent Effects on the acac Ligand. First, the terminal methyl groups of the *acac* ligand were replaced by phenyl groups. This ligand is 1,3-bis(phenyl)propane-1,3-dionate (*bpp* ligand) (Figure 1). The optimized geometries for the ground state and the lowest triplet state show that strong π conjugation between the O−C−C−C−O moiety and phenyl rings, since the π planes of the phenyl rings are closely located on the π plane of the O−C−C−C−O moiety (Figure 2 and Table S2). This strong conjugation energetically pushes down the π^* orbital of the *bpp* ligand and causes effective interaction between the π^* orbitals of the two ligands. This must be the reason why a longer wavelength (546 nm) of the emission peak is obtained for **3** (Table 2). This wavelength is very close to that (545 nm) in *cis*-**1**. Accordingly, it can be said that the replacement of a *thpy* ligand by a *bpp* ligand does not affect the peak wavelength of the emission.

Yagi et al.[88] introduced *n*-butoxy groups to the C3 and C4 sites of the phenyl groups of the *bpp* ligand in order to obtain high solubility for coating processes. Unfortunately, *thpy*Pt-(bdbp) is too large for us to calculate the wavelength of phosphorescence and has too much flexibility of the terminal *n*-butoxy geometries. Methoxy groups, instead of butoxy groups, were thus used in the present study. Table 2 shows the calculated results when one methoxy group is introduced to one of the five sites (C_2−C_6) in each terminal phenyl group: *thpy*Pt(*n*-bmp) (*n* = 2−6) (**5**), where *n*-bmp indicates 1,3-bis(*n*-methoxyphenyl)propane-1,3-dionate (*n* = 2−6, Figure 1 and Figure S1, Supporting Information). The most stable isomer is **5**-**3**, and **5**-**2** and **5**-**4** are less stable than it by only 2−

dx.doi.org/10.1021/jp5046832 | J. Phys. Chem. C 2014, 118, 15412−15421

3 kcal/mol (see Table 1). The most unstable isomers are **5**-**1** and **5**-**5** because of steric effects. Although the geometries of all five isomers are successfully optimized in the present calculations, it is easy to rotate around the C−C bonds between the O−C−C−C−O moieties and the phenyl groups, and it may be difficult to separate **5**-**1** from **5**-**5** and to separate **5**-**2** from **5**-**4** from the viewpoint of synthesis. This speculation is supported by calculated results for the rotational barrier of a terminal methoxyphenyl group; the barriers for the rotation of a methoxyphenyl group are only one kcal/mol in **5**-**1** (**5**-**5**) and 2.3 kcal/mol in **5**-**2** (**5**-**4**) at the DFT level of theory (Figure S2, Supporting Information).

The calculated results show that the introduction of methoxy groups causes small blue shifts (2−12 nm) of the peak wavelengths in all five isomers (Table 2). These results are easily explained as follows: the LUMO mainly has the π^* components of the *thpy* ligand in **2** and **3**, as mentioned above. Even when methoxy groups are introduced into the terminal phenyl groups, the LUMO is rarely affected electronically by the introduction of methoxy groups. Accordingly, even when two methoxy groups are introduced into each phenyl group, it is understandable that the spectral peak wavelength (545 nm) in **4** is almost equal to that in **3** and to that in *cis*-**1** (Table 2).

These results would be true even if *n*-BuO groups are introduced instead of methoxy groups. In fact, Yagi et al.[88] reported that the emission peak appears at the wavelength of 560 nm for *thpy*Pt(bdbp). This peak wavelength seems too short, since the observed wavelength for *btp*Pt(bdbp) is 611 or 613 nm[87,88] and replacement of *thpy* ligand by a 2-2'-(4',5'-benzo)thienyl) pyridinate (*btp*) ligand causes a red shift of about 30 nm as described in the next section. Since the present calculations suggest that the spectral peak appears at the wavelength of 580 nm after correction of the present computational underestimation, the present prediction seems reasonable and is considered to be systematically underestimated and acceptable. Thus, it is proved that introduction of the *bpp*, *bmp*, or *bdmp* (*bdbp*) ligand (or introduction of alkoxy groups into the *bpp* ligand) rarely affects the peak wavelengths of emission.

2.2. Effects of a Benzene Ring Fused to the thpy Ligand. In this section, the effects of a benzene ring fused to the *thpy* ligand are examined for the purpose of obtaining bright red-color emission. It is easy to understand that the extension of π conjugation causes a red shift of spectral peaks, since the π^* orbital (LUMO) mainly has the ligands' π^* character. There are four bonds where a benzene ring can be fused to the *thpy* ligand: [2,2′-(4′,5′-benzo)thienyl)pyridinato-N,$C_{3'}$][2,4-pentanedionato-O,O]platinum(II) [*btp*Pt(acac)] (**6**), [1-(2′-thienyl)isoquinolyl-N,$C_{3'}$][2,4-pentanedionato-O,O]platinum(II) [*1tiq*Pt(acac)] (**7**-**1**), [3-(2′-thienyl)isoquinolyl-N,$C_{3'}$][2,4-pentanedionato-O,O]platinum(II) [*3tiq*Pt(acac)] (**7**-**2**), and [2-(2′-thienyl)quinolyl-N,$C_{3'}$][2,4-pentanedionato-O,O]-platinum(II) [*thq*Pt(acac)] (**7**-**3**) (Figure 1).

The most stable isomer is **6** when a benzene ring is fused to the *thpy* ligand (Table 1). The other three are less stable than this by more than 9 kcal/mol, where DFT tends to underestimate the energy differences among geometrical isomers. The calculated results for emission spectra are shown in Table 2. The emission peaks for **7**-**1**, **7**-**2**, and **7**-**3** are calculated to appear at wavelengths of 538, 531, and 603 nm, respectively. As shown in Figure 2, the LUMO in **2** has large coefficients of π^* orbitals at the *thpy* ligand. The effects of a fused benzene ring can be explained by the π-orbital interaction between a butadiene fragment and the *thpy* ligand. The coefficients at C3′ and C4′ of the *thpy* ligand in the LUMO are large and have the same signs, while those at the terminal carbons in the LUMO of butadiene are also large and have the same signs (Figures 2 and 3). Therefore, the

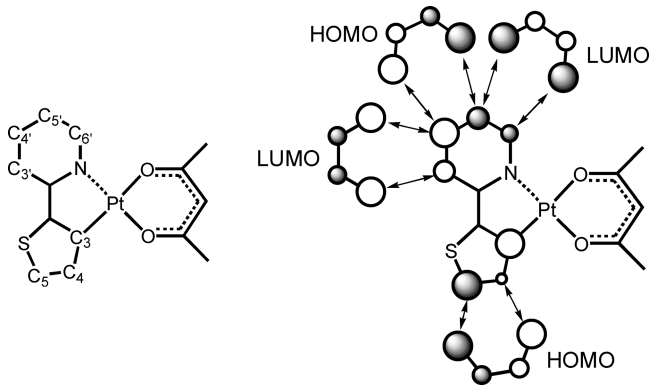

Figure 3. Numbering of atoms in *thpy*Pt(acac) and orbital interactions between *thpy*Pt(acac) and butadiene fragments.

interaction between these vacant orbitals makes the LUMO greatly lowered in energy in **7**-**1** and causes the largest red shift (533 → 603) of the spectral peak in this complex. Similarly, the coefficients at C5′ and C6′ have the same signs, but they are relatively small and steric effects should be considered between the fused ring and an *acac* ligand in **7**-**3**. This might be the reason why a spectral shift rarely occurs in this complex (533 → 538).

The coefficients at C4′ and C5′ of the *thpy* ligand in the LUMO are large and have different signs (Figures 2 and 3). When a butadiene moiety is introduced into the C4′−C5′ bond, the LUMO of the *thpy* ligand interacts strongly with the HOMO, instead of LUMO, of the butadiene moiety. This interaction makes the LUMO energetically lifted and causes a small blue shift of the spectral peak in **7**-**2** (533 → 531).

In **6**, a benzene ring is fused to the C4−C5 bond of **2** (Figure 3). The coefficient at C5 in the LUMO of the *thpy* ligand is large, but that at C4 is rather small and has a different sign. Therefore, the LUMO in **2** weakly interacts with the butadiene moiety, and this interaction cannot explain the red shift (533 → 565) in **6**. The red shift in this complex can be simply explained by the extension of π conjugation. In fact, the LUMO of this complex spreads into the terminal benzene ring as well as the *thpy* moiety of the *btp* ligand. This is evidence of strong interaction of not only LUMO but also other orbitals with the butadiene moiety. The observed peak wavelengths for **6** are located in the wavelength range of 590−612 nm.[49] Since the present computational method underestimates spectral peaks by about 35 nm, the present prediction (600 nm) is included in the wavelength range of observation values (Table 2).

To our knowledge, experimental results have only been reported for the case of the *acac* ligand in **7**-**1** being replaced by a *bdbp* ligand [*1tiq*Pt(bdbp)]: the emission peak of phosphorescence appears at the wavelength of 657 nm.[50] On the basis of the present discussion, since replacement of the *acac* ligand by the *bpp* ligand causes a red shift of 13 nm and the introduction of two methoxy groups has only weak effects on the spectral shift, the emission peak in *1tiq*Pt(bdmp) or *1tiq*Pt(bdbp) is predicted to appear at a wavelength of 651 nm after correcting the underestimation of the present calculations

dx.doi.org/10.1021/jp5046832 | J. Phys. Chem. C 2014, 118, 15412−15421

(about 35 nm). Thus, the present calculations succeeded in explaining the magnitudes of spectral red shifts when a benzene ring is fused to the *thpy* ligand.

Before finishing the present discussion, we should note here that the geometrical displacements were calculated to be 0.02−0.04 Å/atom in the present platinum complexes. These values are comparable with that for *cis*-**1**, and it is therefore understood that fast nonradiative transition would not occur in these complexes.

SUMMARY

Theoretical estimation of the peak wavelengths of phosphorescence was performed at the MCSCF+SOCI/SBKJC+p level of theory for several typical platinum complexes in the research field of OLEDs. The SOC integrals among low-lying electronic states of different spin multiplicities were explicitly calculated within the Z_{eff} approximation. By using these computational methods, the experimental results for peak wavelengths of phosphorescence were reasonably explained for *cis*-**1** and its derivatives: **2**, **3**, **4**, **6**, and **7**.

The replacement of a *thpy* ligand by an *acac* ligand causes a blue shift of the phosphorescent peak by about 10 nm, while the introduction of a *bpp*, *bmp*, or *bdmp* ligand has almost no effect on the peak wavelength of phosphorescence. When a benzene ring is fused to a *thpy* ligand in *thpy*Pt(acac), the peak wavelength is calculated to be 565 (**6**) or 603 (**7**-**1**) nm. Accordingly, if a benzene ring is fused to a *thpy* ligand in *thpy*Pt(bdmp), a spectral peak is predicted to appear at the wavelength of 613 or 651 nm for *btp*Pt(bdbp) and *1tiq*Pt(bdbp) after correction of the present computational underestimation. These predictions are consistent with experimental results reported so far.[49,50,87−89] Based on the success of the present calculations, investigation of bis[2-phenylpyridinato]-platinum [$Pt(ppy)_2$] and its derivatives is now being performed in our laboratory.

ASSOCIATED CONTENT

Supporting Information

The names of platinum complexes are shown in Table S1. The Cartesian coordinates of platinum complexes are available (Table S2). The geometrical structures optimized for the lowest triplet states are illustrated in Figure S1, and the transition-state geometries for the rotation of *n*-methoxyphenyl groups (n = 2 and 3) are depicted in Figure S2. This material is available free of charge via the Internet at http://pubs.acs.org.

AUTHOR INFORMATION

Corresponding Author

*E-mail: shiro@c.s.osakafu-u.ac.jp. Tel: +81-72-254-9702.

Notes

The authors declare no competing financial interest.

REFERENCES

(1) Baldo, M. A.; O'Brien, D. F.; You, Y.; Shoustikov, A.; Sibley, S.; Thompson, M. E.; Forrest, S. R. Highly Efficient Phosphorescent Emission from Organic Electroluminescent Devices. *Nature (London)* **1998**, *395*, 151−154.

(2) Baldo, M. A.; O'Brien, D. F.; Thompson, M. E.; Forrest, S. R. Excitonic Singlet−Triplet Ratio in a Semiconducting Organic Thin Film. *Phys. Rev. B* **1999**, *60*, 14422−14428.

(3) O'Brien, D. F.; Baldo, M. A.; Thompson, M. E.; Forrest, S. R. Improved Energy Transfer in Electrophosphorescent Devices. *Appl. Phys. Lett.* **1999**, *74*, 442−444.

(4) Adachi, C.; Baldo, M. A.; Forrest, S. R. High-Efficiency Organic Electrophosphorescent Devices with Tris(2-phenylpyridine)iridium Doped into Electron-Transporting Materials. *Appl. Phys. Lett.* **2000**, *77*, 904−906.

(5) Ikai, M.; Tokito, S.; Sakamoto, Y.; Suzuki, T.; Taga, Y. Highly Efficient Phosphorescence from Organic Light-Emitting Devices with an Exciton-Block Layer. *Appl. Phys. Lett.* **2000**, *79*, 156−158.

(6) Tokito, S.; Iijima, T.; Tsuzuki, T.; Sato, F. High-Efficiency White Phosphorescent Organic Light-Emitting Devices with Greenish-Blue and Red-Emitting Layers. *Appl. Phys. Lett.* **2003**, *83*, 2459−2461.

(7) Wang, Y.; Herron, N.; Grushin, V. V.; LeCloux, D. D.; Petrov, V. A. Highly Efficient Electroluminescent Materials Based on Fluorinated Organometallic Iridium Compounds. *Appl. Phys. Lett.* **2001**, *79*, 449−451.

(8) Adachi, C.; Kwong, R. C.; Djurovich, P.; Adamovich, V.; Baldo, M. A.; Thompson, M. E.; Forrest, S. R. Endothermic Energy Transfer: A Mechanism for Generating Very Efficient High-Energy Phosphorescent Emission in Organic Materials. *Appl. Phys. Lett.* **2001**, *79*, 2082−2084.

(9) Grushin, V. V.; Herron, N.; LeCloux, D. D.; Marshall, W. J.; Petrov, V. A.; Wang, Y. New, Efficient Electroluminescent Materials Based on Organometallic Ir Complexes. *Chem. Commun.* **2001**, 1494−1495.

(10) Ostrowski, J. C.; Robinson, M. R.; Heeger, A. J.; Bazan, C. C. Amorphous Iridium Complexes for Electrophosphorescent Light Emitting Devices. *Chem. Commun.* **2002**, 784−785.

(11) Holmes, R. J.; Forrest, S. R.; Tung, Y.-J.; Kwong, R. C.; Brown, J. J.; Garon, S.; Thompson, M. E. Blue Organic Electrophosphorescence Using Exothermic Host−Guest Energy Transfer. *Appl. Phys. Lett.* **2003**, *82*, 2422−2424.

(12) Cheng, G.; Li, F.; Duan, Y.; Feng, J.; Liu, S.; Qiu, S.; Lin, D.; Ma, Y.; Lee, S. T. White Organic Light-Emitting Devices Using a Phosphorescent Sensitizer. *Appl. Phys. Lett.* **2003**, *82*, 4224−4226.

(13) Holmes, R. J.; D'Andrade, M. W.; Forrest, S. R.; Ren, X.; Li, J.; Thompson, M. E. Efficient, Deep-Blue Organic Electrophosphorescence by Guest Charge Trapping. *Appl. Phys. Lett.* **2003**, *83*, 3818−3820.

(14) Karatsu, T.; Nakamura, T.; Yagai, S.; Kitamura, A.; Yamaguchi, K.; Matsushima, Y.; Iwata, T.; Hori, Y.; Hagiwara, T. Photochemical mer → fac One-way Isomerization of Phosphorescent Material. Studies by Time-Resolved Spectroscopy for Tris[2-(4′,6′-difluorophenyl) pyridine] iridium(III) in Solution. *Chem. Lett.* **2003**, *10*, 886−887.

(15) Kawamura, Y.; Goushi, K.; Brooks, J.; Brown, J. J.; Sasabe, H.; Adachi, C. 100% Phosphorescence Quantum Efficiency of Ir(III) Complexes in Organic Semiconductor Films. *Appl. Phys. Lett.* **2005**, *86*, 071104.

(16) Colombo, M. G.; Brunold, T. C.; Riedener, T.; Güdel, H. U.; Förtsch, M.; Bürgi, H.-B. Facial Tris Cyclometalated Rhodium(3+) and iridium(3+) complexes: their synthesis, structure, and optical spectroscopic properties. *Inorg. Chem.* **1994**, *33*, 545−550.

(17) Baldo, M. A.; Lamansky, S.; Burrows, P. E.; Thompson, M. E.; Forrest, S. R. Very High-Efficiency Green Organic Light-Emitting Devices Based on Electrophosphorescence. *Appl. Phys. Lett.* **1999**, *75*, 4−6.

(18) Adachi, C.; Baldo, M. A.; Forrest, S. R.; Lamansky, S.; Thompson, M. E.; Kwong, R. C. High-Efficiency Red Electrophosphorescence Devices. *Appl. Phys. Lett.* **2001**, *78*, 1622−1624.

(19) Adachi, C.; Baldo, M. A.; Thompson, M. E.; Forrest, S. R. Nearly 100% Internal Phosphorescence Efficiency in an Organic Light-Emitting Device. *J. Appl. Phys.* **2001**, *90*, 5048−5051.

(20) Lamansky, S.; Djurovich, P.; Murphy, D.; Abdel-Razzaq, F.; Lee, H.-E.; Adachi, C.; Burrows, P. E.; Forrest, S. R.; Thompson, M. E. Highly Phosphorescent Bis-Cyclometalated Iridium Complexes: Synthesis, Photophysical Characterization, and Use in Organic Light Emitting Diodes. *J. Am. Chem. Soc.* **2001**, *123*, 4304−4312.

(21) Tamayo, A. B.; Alleyne, B. D.; Djurovich, P. I.; Lamansky, S.; Tsyba, I.; Ho, N. N.; Bau, R.; Thompson, M. E. Synthesis and

Characterization of Facial and Meridional Tris-cyclometalated Iridium-(III) Complexes. *J. Am. Chem. Soc.* **2003**, *125*, 7377−7378.
(22) Finkenzeller, W. J.; Yersin, H. Emission of Ir(ppy)3. Temperature Dependence, Decay Dynamics, and Magnetic Field Properties. *Chem. Phys. Lett.* **2003**, *377*, 299−305.
(23) Tsuboyama, A.; Iwawaki, H.; Furugoi, M.; Mukaide, T.; kamatani, J.; Igawa, S.; Moriyama, T.; Miura, S.; Takiguchi, T.; Okada, S.; Hoshino, M.; Ueno, K. Homoleptic Cyclometalated Iridium Complexes with Highly Efficient Red Phosphorescence and Application to Organic Light-Emitting Diode. *J. Am. Chem. Soc.* **2003**, *125*, 12971−12979.
(24) Tang, K.-C.; Liu, K. L.; Chen, I.-C. Rapid Intersystem Crossing in Highly Phosphorescent Iridium Complexes. *Chem. Phys. Lett.* **2004**, *386*, 437−441.
(25) Stampor, W.; Mezù yk, J.; Kalinowski, J. Electroabsorption Study of Metal-to-Ligand Charge Transfer in an Organic Complex of Iridium (III). *Chem. Phys.* **2004**, *300*, 189−195.
(26) Goushi, K.; Kawamura, Y.; Sasabe, H.; Adachi, C. Unusual Phosphorescence Characteristics of Ir(ppy)3 in a Solid Matrix at Low Temperatures. *Jpn. J. Appl. Phys.* **2004**, *43*, L937−939.
(27) Cocchi, M.; Fattori, V.; Virgili, D.; Sabatini, C.; Di Marco, P.; Maestri, M.; Kalinowski, J. Highly Efficient Organic Electrophosphorescent Light-Emitting Diodes with a Reduced Quantum Efficiency Roll off at Large Current Densities. *Appl. Phys. Lett.* **2004**, *84*, 1052−1054.
(28) Holzer, W.; Penzkofer, A.; Tsuboi, T. Absorption and Emission Spectroscopic Characterization of $Ir(ppy)_3$. *Chem. Phys.* **2005**, *308*, 93−102.
(29) Kobayashi, T.; Ide, N.; Matsusue, N.; Naito, H. Temperature Dependence of Photoluminescence Lifetime and Quantum Efficiency in Neat fac-Ir(ppy)3 Thin Films. *Jpn. J. Appl. Phys.* **2005**, *44*, 1966−1969.
(30) Gu, X.; Fei, T.; Zhang, H.; Xu, H.; Yang, B.; Ma, Y.; Liu, X. Theoretical Studies of Blue-Emitting Iridium Complexes with Different Ancillary Ligands. *J. Phys. Chem. A* **2008**, *112*, 8387−8393.
(31) Rausch, A. F.; Thompson, M. E.; Yersin, H. Matrix Effects on the Triplet State of the OLED Emitter $Ir(4,6\text{-}dFppy)_2(pic)$ (FIrpic): Investigations by High-Resolution Optical Spectroscopy. *Inorg. Chem.* **2009**, *48*, 1928−1937.
(32) Baranoff, E.; Curchod, B. F. E.; Frey, J.; Scopelliti, R.; Kessler, F.; Tavernelli, I.; Rothlisberger, U.; Grätzel, M.; Nazeeruddin, M. K. Acid-Induced Degradation of Phosphorescent Dopants for OLEDs and Its Application to the Synthesis of Tris-heteroleptic Iridium(III) Bis-cyclometalated Complexes. *Inorg. Chem.* **2012**, *51*, 215−224.
(33) Chassot, L.; Müller, E.; von Zelewsky, A. cis-Bis(2-phenylpyridine)platinum(II) (CBPPP): A Simple Molecular Platinum Compound. *Inorg. Chem.* **1984**, *23*, 4249−4253.
(34) Bonafede, S.; Ciano, M.; Bolletta, F.; Balzani, V.; Chassot, L.; von Zelewsky, A. Electrogenerated Chemiluminescence of an ortho-Metalated Platinum(II) Complex. *J. Phys. Chem.* **1986**, *90*, 3836−3841.
(35) Sandrini, D.; Maestri, M.; Balzani, V.; Chassot, L.; von Zelewsky, A. Photochemistry of the Orthometalated cis-Bis[2-(2-thienyl)-pyridine]platinum(II) Complex in Halocarbon Solvents. *J. Am. Chem. Soc.* **1987**, *109*, 7720−7724.
(36) Chassot, L.; von Zelewsky, A. Cyclometalated Complexes of Platinum(II): Homoleptic Compounds with Aromatic C,N Ligands. *Inorg. Chem.* **1987**, *26*, 2814−2818.
(37) Barigelletti, F.; Sandrini, D.; Maestri, M.; Balzani, V.; von Zelewsky, A.; Chassot, L.; Jolliet, P.; Maeder, U. Temperature Dependence of the Luminescence of Cyclometalated Palladium(II), Rhodium(III), Platinum(II), and Platinum(IV) Complexes. *Inorg. Chem.* **1988**, *27*, 3644−3647.
(38) Jolliet, P.; Gianini, M.; von Zelewsky, A.; Bernardinelli, G.; Stoeckly-Evans, H. Cyclometalated complexes of palladium(II) and platinum(II): cis-Configured homoleptic and heteroleptic compounds with aromatic C-N ligands. *Inorg. Chem.* **1996**, *35*, 4883−4888.
(39) Cummings, S. D.; Eisenberg, R. Tuning the Excited-State Properties of Platinum(II) Diimine Dithiolate Complexes. *J. Am. Chem. Soc.* **1996**, *118*, 1949−1960.
(40) Büchner, R.; Field, J. S.; Haines, R. J.; Cunningham, C. T.; McMillin, D. R. Luminescence Properties of Salts of the [Pt(trpy)Cl]+ and $[Pt(trpy)(MeCN)]_2$ + Chromophores: Crystal Structure of $[Pt(trpy)(MeCN)](SbF_6)_2$. *Inorg. Chem.* **1997**, *36*, 3952−3956.
(41) Schmidt, J.; Strasser, J.; Yersin, H. Determination of Relaxation Paths in the Manifold of Excited States of $Pt(2\text{-}thpy)_2$ and $[Ru(bpy)_3]_2$ + by Time-Resolved Excitation and Emission. *Inorg. Chem.* **1997**, *36*, 3957−3965.
(42) Donges, D.; Nagle, J. K.; Yersin, H. Intraligand charge transfer in Pt(qol)(2). Characterization of electronic states by high-resolution Shpol'skii spectroscopy. *Inorg. Chem.* **1997**, *36*, 3040−3048.
(43) Strasser, J.; Donges, D.; Humbs, W.; Kulikova, M. V.; Balashev, K. P.; Yersin, H. Dynamical Processes between Triplet Sublevels of Metal−Organic Pt(II) Compounds. *J. Lumin.* **1998**, *76*−*77*, 611−614.
(44) Shoustikov, A. A.; You, Y.; Thompson, M. E. Electroluminescence Color Tuning by Dye Doping in Organic Light-Emitting Diodes. *IEEE J. Sel. Top. Quantum Electron.* **1998**, *4*, 3.
(45) Pier; Pierloot, K.; Ceulemans, A.; Merchán, M.; Serrano-Andrés, L. Electronic Spectra of the Cyclometalated Complexes $M(2\text{-}thienylpyridine)_2$ with M = Pd, Pt: A Theoretical Study. *J. Phys. Chem. A* **2000**, *104*, 4374−4382.
(46) Lamansky, S.; Kwong, R. C.; Nugent, M.; Djurovich, P. I.; Thompson, M. E. Molecularly Doped Polymer Light Emitting Diodes Utilizing Phosphorescent Pt(II) and Ir(III) Dopants. *Org. Electron.* **2001**, *2*, 53−62.
(47) Lu, W.; Chan, M. C. W.; Cheung, K.-K.; Che, C.-M. $\pi-\pi$ Interactions in Organometallic Systems. Crystal Structures and Spectroscopic Properties of Luminescent Mono-, Bi-, and Trinuclear Trans-cyclometalated Platinum(II) Complexes Derived from 2,6-Diphenylpyridine. *Organometallics* **2001**, *20*, 2477−2486.
(48) Lu, W.; Mi, B.-X.; Chan, M. C. W.; Hui, Z.; Zhu, N.; Lee, S.-T.; Che, C.-M. $[(CNN)Pt(CC)_nR]$ (HCNN = 6-aryl-2,2′-bipyridine, n =1−4, R = aryl, $SiMe_3$) as a New Class of Light-Emitting Materials and Their Applications in Electrophosphorescent Devices. *Chem. Commun.* **2002**, 206−207.
(49) Brooks, J.; Babayan, Y.; Lamansky, S.; Djurovich, P. I.; Tsybam, I.; Bau, R.; Thompson, M. E. Synthesis and Characterization of Phosphorescent Cyclometalated Platinum Complexes. *Inorg. Chem.* **2002**, *41*, 3055−3066.
(50) Kozhevnikov, D. N.; Kozhevnikov, V. N.; Ustinova, M. M.; Santoro, A.; Bruce, D. W.; Koenig, B.; Czerwieniec, R.; Fischer, T.; Zabel, M.; Yersin, H. Synthesis of Cyclometallated Platinum Complexes with Substituted Thienylpyridines and Detailed Characterization of Their Luminescence Properties. *Inorg. Chem.* **2009**, *48*, 4179−4189.
(51) Lin, Y.-Y.; Chan, S.-C.; Chan, M. C. W.; Hou, Y.-J.; Zhu, N.; Che, C.-M.; Liu, Y.; Wang, Y. Structural, photophysical, and electrophosphorescent properties of platinum(II) complexes supported by tetradentate N_2O_2 chelates. *Chem.—Eur. J.* **2003**, *9*, 1263−1272.
(52) Osad'ko, I. S.; Lobanov, A. N. Phosphorescence studies of the Pt(thpy)(2) complex for use in single molecule spectroscopy. *Opt. Spectrosc.* **2005**, *88*, 297−300.
(53) Minaev, B. F.; Knuts, S.; Agren, H.; Vahtras, O. The vibronically induced phosphorescence in benzene. *Chem. Phys.* **1993**, *175*, 245−254.
(54) Agren, H.; Vahtras, O.; Minaev, B. F. Response Theory and Calculations of Spin−Orbit Coupling Phenomena in Molecules. *Adv. Quantum Chem.* **1996**, *27*, 71−162.
(55) Minaev, B. F. Intensity of Singlet−Triplet Transitions in C_{60} Fullerene Calculated on the Basis of the Time-Dependent Density Functional Theory and Taking into Account the Quadratic Response. *Opt. Spectrosc.* **2005**, *98* (3), 336−340.
(56) Minaev, B. F.; Jansson, E.; Ågrena, H.; Schrader, S. Theoretical study of phosphorescence in dye doped light emitting diodes. *J. Chem. Phys.* **2006**, *125*, 234704−1∼18.
(57) Jansson, E.; Minaev, B.; Schrader, S.; Ågren, H. Time-Dependent Density Functional Calculations of Phosphorescence

Parameters for fac-Tris(2-phenylpyridine)Iridium. *Chem. Phys.* **2007**, *333*, 157−167.
(58) Minaev, B.; Minaeva, V.; Ågren, H. Theoretical Study of the Cyclometalated Iridium(III) Complexes Used as Chromophores for Organic Light-Emitting Diodes. *J. Phys. Chem. A* **2009**, *113*, 726−735.
(59) Minaev, B.; Ågren, H.; De Angelis, F. Theoretical Design of Phosphorescence Parameters for Organic Electro-luminescence Devices Based on Iridium Complexes. *Chem. Phys.* **2009**, *358*, 245−257.
(60) Li, X.; Minaev, B.; Ågren, H.; Tian, H. Density Functional Theory Study of Photophysical Properties of Iridium(III) Complexes with Phenylisoquinoline and Phenylpyridine Ligands. *J. Phys. Chem. C* **2011**, *115*, 20724−20731.
(61) Li, X.; Minaev, B.; Ågren, H.; Tian, H. Theoretical Study of Phosphorescence of Iridium Complexes with Fluorine-Substituted Phenylpyridine Ligands. *Eur. J. Inorg. Chem.* **2011**, 2517−2524.
(62) Volyniuk, D.; Cherpak, V.; Stakhira, p.; Minaev, B. F.; Baryshnikov, G. V.; Chapran, M.; Tomkeviciene, A.; Keruckas, J.; Grazulevicius, J. V. Highly Efficient Blue OLEDs Based on Intermolecular Triplet-Singlet Energy Transfer. *J. Phys. Chem. C* **2013**, *117*, 22538−22544.
(63) Minaev, B. F.; Baryshnikov, G.; Agren, H. Principles of Phosphorescent Organic Light Emitting Devices. *Phys. Chem. Chem. Phys.* **2013**, *16*, 1719−1758.
(64) Cherpak, V.; Stakhira, P.; Minaev, B.; Baryshnikov, G.; Stromylo, E.; Helzhynskyy, I.; Chapran, M.; Volyniuk, D.; Tomkuté-Lukšiené, D.; Malinauskas, T.; Getautis, V.; Tomkeviciene, A.; Simokaitiene, J.; Grazulevicius, J. V. Efficient "Warm-White" OLEDs Based on the Phosphorescent bis-2 Cyclometalated iridium(III) Complex. *J. Phys. Chem. C* **2014**, *118*, 11271−11278.
(65) Matsushita, T.; Asada, T.; Koseki, S. Relativistic Study on Fluorescence and Phosphorescence Emitted by Palladium and Platinum Complexes. *J. Phys. Chem. A* **2006**, *110*, 13295−13302.
(66) Matsushita, T.; Asada, T.; Koseki, S. Relativistic Study on Emission Mechanism in Tris-(2-phenylpyridine)-Iridium. *J. Phys. Chem. C* **2007**, *111*, 6897−6903.
(67) Koseki, S.; Kamata, N.; Asada, T.; Yagi, S.; Nakazumi, H.; Matsushita, T. Spin−Orbit Coupling Analyses of the Geometrical Effects on Phosphorescence in $Ir(ppy)_3$ and Its Derivatives. *J. Phys. Chem. C* **2013**, *117*, 5314−5327. It should be noted that the equation in our previous paper (ref 67) is wrong. After the mass centers of the geometries optimized for the ground state and the lowest triplet state are moved to the coordinate origin and the orientation of the complexes is aligned under the condition that rotational angular momentum should not be generated by geometrical displacement between the optimized geometries of the two states, the geometrical displacement is defined as $|\Delta Q| = \frac{1}{N}\sum_{i=1}^{N}\sqrt{\sum_{\alpha}^{x,y,z}\left(q_{i,\alpha}^{S0} - q_{i,\alpha}^{T1}\right)^2}$ (N being the number of atoms).
(68) Schmidt, M. W.; Gordon, M. S. The Construction and Interpretation of MCSCF Wavefunctions. *Annu. Rev. Phys. Chem.* **1998**, *49*, 233−266.
(69) Koseki, S.; Ishihara, Y.; Umeda, H.; Fedorov, D. G.; Gordon, M. S. Dissociation Potential Curves of Low-Lying States in Transition Metal Hydrides. I. Hydrides of Group 4. *J. Phys. Chem. A* **2002**, *106*, 785−794.
(70) Koseki, S.; Ishihara, Y.; Umeda, H.; Fedorov, D. G.; Schmidt, M. W.; Gordon, M. S. Dissociation Potential Curves of Low-Lying States in Transition Metal Hydrides. II. Hydrides of Groups 3 and 5. *J. Phys. Chem. A* **2004**, *108*, 4707−4719.
(71) Koseki, S.; Matsushita, T.; Gordon, M. S. Dissociation Potential Curves of Low-Lying States in Transition Metal Hydrides. III. Hydrides of Groups 6 and 7. *J. Phys. Chem. A* **2006**, *110*, 2560−2570.
(72) Langhoff, S. R. Theoretical Treatment of the Spin−Orbit Coupling in the Rare Gas Oxides NeO, ArO, KrO, and XeO. *J. Chem. Phys.* **1980**, *73*, 2379−2386 and references therein.
(73) Koseki, S. Spin−Orbit Coupling Effects in Di-hydrides of Third-Row Transition Elements. In *Computational Methods in Sciences and Engineering, Theory and Computation: Old Problems and New Challenges*; Maroulis, G., Simos, T., Eds.; AIP: New York, 2008; CP963, Vol. *1*, pp 257−267.
(74) Koseki, S.; Shimakura, N.; Fujimura, Y.; Asada, T.; Kono, H. Spin−Orbit Coupling Effects in Dihydrides of Third-Row Transition Elements II. Interplay of Nonadiabatic Coupling in Dissociation Path of Rhenium Dihydride. *J. Chem. Phys.* **2009**, *131*, 044122−1−8.
(75) Hisashima, T.; Matsushita, T.; Asada, T.; Koseki, S. Tetra-hydrides of the Third-Row Transition Elements: Spin−Orbit Coupling Effects on Geometrical Deformation in WH_4 and OsH_4. *Theor. Chem. Acc.* **2008**, *120*, 85−94.
(76) Koseki, S.; Hisashima, T.; Asada, T.; Toyota, A.; Matsunaga, N. Tetra-hydrides of the Third-Row Transition Elements: Spin−Orbit Coupling Effects to the Stability of Rhenium Tetra-hydride. *J. Chem. Phys.* **2010**, *133*, 174112−1−9.
(77) Koseki, S.; Schmidt, M. W.; Gordon, M. S. MCSCF/6-31G(d,p) Calculations of One-Electron Spin−Orbit Coupling Constants in Diatomic Molecules. *J. Phys. Chem.* **1992**, *96*, 10768−10772.
(78) Koseki, S.; Gordon, M. S.; Schmidt, M. W.; Matsunaga, N. Main Group Effective Nuclear Charges for Spin−Orbit Calculations. *J. Phys. Chem.* **1995**, *99*, 12764−12772.
(79) Matsunaga, N.; Koseki, S.; Gordon, M. S. Relativistic Potential Energy Surfaces of XH_2 (X = C, Si, Ge, Sn, and Pb) Molecules: Coupling of $^1A_1$ and $^3B_1$ States. *J. Chem. Phys.* **1996**, *104*, 7988−7996.
(80) Koseki, S.; Schmidt, M. W.; Gordon, M. S. Effective Nuclear Charges for the First- Through Third-Row Transition Metal Elements in Spin−Orbit Calculations. *J. Phys. Chem. A* **1998**, *102*, 10430−10435.
(81) Koseki, S.; Fedorov, D. G.; Schmidt, M. W.; Gordon, M. S. Spin−Orbit Splittings in the Third-Row Transition Elements: Comparison of Effective-Nuclear-Charge and Full Breit−Pauli Calculations. *J. Phys. Chem. A* **2001**, *105*, 8262−8268.
(82) Fedorov, D. G.; Koseki, S.; Schmidt, M. W.; Gordon, M. S. Spin−Orbit Coupling in Molecules: Chemistry beyond the Adiabatic Approximation. *Int. Rev. Phys. Chem.* **2003**, *22*, 551−592.
(83) Fedorov, D. G.; Schmidt, M. W.; Koseki, S.; Gordon, M. S. Spin−Orbit Coupling Methods and Applications to Chemistry. In Recent Advances in Relativistic Molecular Theory. *Recent Advances in Relativistic Molecular Theory*; World Scientific: Singapore, 2004; Vol. *5*, pp 107−136.
(84) Finkenzeller, W. J.; Thompson, M. E.; Yersin, H. Phosphorescence Dynamics and Spin-Lattice Relaxation of the OLED Emitter $Ir(btp)_2(acac)$. *Chem. Phys. Lett.* **2007**, *444*, 273−279.
(85) Rausch, A. F.; Thompson, M. E.; Yersin, H. Blue Light Emitting Ir(III) Compounds for OLEDs - New Insights into Ancillary Ligand Effects on the Emitting Triplet State. *J. Phys. Chem. A* **2009**, *113*, 5927−5932.
(86) Rausch, A. F.; Thompson, M. E.; Yersin, H. Triplet State Relaxation Processes of the OLED Emitter Pt(4,6-dFppy)(acac). *Chem. Phys. Lett.* **2009**, *468*, 46−51.
(87) Tsujimoto, H.; Yagi, S.; Honda, Y.; Terao, H.; Maeda, T.; Nakazumi, H.; Sakurai, Y. Photoluminescent Properties of Heteroleptic Cyclometalated Platinum(II) Complexes Bearing 1,3-bis(3,4-Dibutoxyphenyl)Propane-1,3-Dionate as an Ancillary Ligand. *J. Lumin.* **2010**, *130*, 217−221.
(88) Tsujimoto, H.; Sakurai, Y.; Yagi, S.; Honda, Y.; Asuka, H.; Terao, H.; Maeda, T.; Nakazumi, H. Pure Red Electroluminescence from Novel Heteroleptic Cyclometalated Platinum(II) Emitters Embedded in Polyvinylcarbazole. *Synth. Met.* **2010**, *160*, 615−620.
(89) Tsujimoto, H.; Yagi, S.; Asuka, H.; Inui, Y.; Ikawa, S.; Maeda, T.; Nakazumi, H.; Sakurai, Y. Pure red electrophosphorescence from polymer light-emitting diodes doped with highly emissive bis-cyclometalated iridium(III) complexes. *J. Organomet. Chem.* **2010**, *695*, 1972−1978.
(90) Lin, H.; Truhlar, D. G. QM/MM: What Have We Learned, Where Are We, and Where Do We Go from Here? *Theor. Chem. Lett.* **2007**, *117*, 185−199.
(91) Bhattacharyya, S.; Stankovich, M. T.; Truhlar, D. G.; Gao, J. Combined Quantum Mechanical and Molecular Mechanical Simulations of One- and Two-Electron Reduction Potentials of Flavin

Cofactor in Water, Medium-Chain Acyl-CoA Dehydrogenase, and Cholesterol Oxidase. *J. Phys. Chem. A* **2007**, *111*, 5729−5742.
(92) Svenssion, M.; Humbel, S.; Froese, R. D. J.; Matsubara, T.; Sieber, S.; Morokuma, K. ONIOM: A Multilayered Integrated MO + MM Method for Geometry Optimizations and Single Point Energy Predictions. A Test for Diels−Alder Reactions and $Pt(P(t\text{-}Bu)_3)_2 + H_2$ Oxidative Addition. *J. Phys. Chem.* **1996**, *100*, 19357−19363.
(93) Dapprich, S.; Komaromi, I.; Byun, K. S.; Morokuma, K.; Frisch, M. J. A New ONIOM Implementation in Gaussian98. Part I. The Calculation of Energies, Gradients, Vibrational Frequencies and Electric Field Derivatives. *THEOCHEM* **1999**, *462*, 1−21.
(94) Vreven, T.; Mennucci, B.; da Silva, C. O.; Morokuma, K.; Tomasi, J. The ONIOM-PCM Method: Combining the Hybrid Molecular Orbital Method and the Polarizable Continuum Model for Solvation. Application to the Geometry and Properties of a Merocyanine in Solution. *J. Chem. Phys.* **2001**, *115*, 62−72.
(95) Eichler, U.; Kölmel, C. M.; Sauer, J. Combining ab initio Techniques with Analytical Potential Functions for Structure Predictions of Large Systems: Method and Application to Crystalline Silica Polymorphs. *J. Comput. Chem.* **1996**, *18*, 463−477.
(96) Asada, T.; Takahashi, T.; Koseki, S. Theoretical Study of Environmental Effects for Proton Transfer Reaction Through the Peptide Bond in a Model System. *Theor. Chem. Acc.* **2008**, *120*, 263−271.
(97) Asada, T.; Nagase, S.; Nishimoto, K.; Koseki, S. Molecular Dynamics Simulation Study on Stabilities and Reactivities of NADH Cytochrom B5 Reductase. *J. Phys. Chem. B* **2008**, *112*, 5718−5727.
(98) Asada, T.; Nagase, S.; Nishimoto, K.; Koseki, S. Simulation Study of Interactions and Reactivities between NADH Cytochrom b5 Reductase and Cytochrom b5. *J. Mol. Liq.* **2009**, *147*, 139−144.
(99) Asada, T.; Hamamura, S.; Matsushita, T.; Koseki, S. Theoretical Study on the Absorption Spectra of fac-$Ir(ppy)_3$ in the Amorphous Phase of Organic Electro-Luminescent Devices. *Res. Chem. Intermed.* **2009**, *35*, 851−863.
(100) Koseki, S.; Asada, T.; Matsushita, T. Phosphorescent Materials for Organic Electro-Luminescent Devices. *J. Comput. Theoret. Nanoscience* **2009**, *6*, 1352−1360.
(101) Asada, T.; Ohta, K.; Matsushita, T.; Koseki, S. QM/MM Investigation on the Degradation Mechanism of the Electron-Transporting Layer. *Theor. Chem. Acc.* **2011**, *130*, 439−448.
(102) Becke, A. D. Density-Functional Thermochemistry. III. The Role of Exact Exchange. *J. Chem. Phys.* **1993**, *98*, 5648−5652.
(103) Stevens, W. J.; Basch, H.; Krauss, M.; Jasien, P. Relativistic Compact Effective Potentials and Efficient, Shared-Exponent Basis Sets for the Third-, Fourth-, and Fifth-Row Atoms. *Can. J. Chem.* **1992**, *70*, 612−630.
(104) Cundari, T. R.; Stevens, W. J. Effective Core Potential Methods for the Lanthanides. *J. Chem. Phys.* **1993**, *98*, 5555−5565.
(105) Exponents of 0.993 are used for *f* functions on Pt. The *d* exponents are 0.650 (S) and 0.800 (C and N). The *p* exponents are 1.100 (H). This basis set is referred to as SBKJC+p.
(106) Lengsfield, B. H., III; Jafri, J. A.; Phillips, D. H.; Bauschlicher, C. W., Jr. On the Use of Corresponding Orbitals in the Calculation of Nonorthogonal Transition Moments. *J. Chem. Phys.* **1981**, *74*, 6849−6856.
(107) Schmidt, M. W.; Baldridge, K. K.; Boatz, J. A.; Elbert, S. T.; Gordon, M. S.; Jensen, J. H.; Koseki, S.; Matsunaga, N.; Nguyen, K. A.; Su, S.; Windus, T. L.; Dupuis, M.; Montgomery, J. A., Jr. General Atomic and Molecular Electronic Structure System (GAMESS). *J. Comput. Chem.* **1993**, *14*, 1347−1363.
(108) The energy difference between the cis and trans isomer is calculated to be 7.6 (DFT), 11.5 (MCSCF), 9.9 (MCSCF+SOCI), 9.7 (MCSCF+SOCI+SOC), or 20.7 (MCQDPT2) kca/mol.
(109) Colbert, D. T.; Miller, W. H. A Novel Discrete Variable Representation for Quantum-Mechanical Reactive Scattering via the S-Matrix Kohn Method. *J. Chem. Phys.* **1992**, *96*, 1982−1991.
(110) Matsushita, T. Thesis; Development of Theoretical Methods for Material Design; Osaka Prefecture University, 2007.
(111) Koseki, S.; Gordon, M. S. Potential Energy Surfaces and Dynamical Properties of Three Low Lying States of Silylene. *J. Mol. Spectrosc.* **1987**, *123*, 392−404.
(112) Furlani, T. R.; King, H. F. Theory of Spin-Orbit-Coupling − Application to Singlet-Triplet Interaction in the Trimethylene Biradical. *J. Chem. Phys.* **1985**, *82*, 5577−5583.
(113) Carlacci, L.; Doubleday, C.; Furlani, T. R.; King, H. F.; McIver, J. W. Spin-Orbit-Coupling in Biradicals − Ab Initio MCSCF Calculations on Trimethylene and the Methyl Methyl Radical Pair. *J. Am. Chem. Soc.* **1987**, *109*, 5323−5329.
(114) Caldwell, R. A.; Carlacci, L.; Doubleday, C. E.; King, H. F.; McIver, J. W. Viable Geometries for T1-S0 ISC in Alkene Triplets. *J. Am. Chem. Soc.* **1988**, *110*, 6901−6903.
(115) King, H. F.; Furlani, T. R. Computation of One-Electron and 2-Electron Spin-Orbit Integrals. *J. Comput. Chem.* **1988**, *9*, 771−778.